Effect of a Sawtooth Boundary on Couette Flow

Gabriel Mateescu
Department of Computer Science, Virginia Polytechnic Institute & State University, Blacksburg, VA 24061, U.S.A.

C.-Y. Wang
Departments of Mathematics and Mechanical Engineering, Michigan State University, East Lansing, MI 48824, U.S.A.

Calvin J. Ribbens
Department of Computer Science, Virginia Polytechnic Institute & State University, Blacksburg, VA 24061, U.S.A.

and

Layne T. Watson
Departments of Computer Science and Mathematics, Virginia Polytechnic Institute & State University, Blacksburg, VA 24061, U.S.A.

Abstract—The relative tangential motion of a smooth plate and a corrugated plate separated by a viscous fluid is studied. The full Navier-Stokes equations are solved using Hermite collocation and Newton's method. Detailed streamlines and vorticity distributions are determined. The increased drag due to corrugation is found to be substantial.

1. INTRODUCTION

One of the most basic flows in fluid mechanics is Couette flow, the shear flow between parallel surfaces in relative tangential motion. Couette flow occurs in every fluid machinery involving moving parts and is especially important for hydrodynamic lubrication. If the surfaces are smooth and flat, the solution is the simple linear velocity distribution, with a drag proportional to the relative velocity and inversely proportional to the gap width. We ask, what is the flow and drag if the surface is not flat but striated? These striations, or roughness, may be caused by rough milling or planing processes, or may be intentional, such as in entrapment of lubricants or the enhancement of heat or mass transfer [1] [2].

There has been little theoretical work on Couette flow with striated boundaries, due to the complicated boundary conditions. If the protuberances have large wavelength to amplitude ratios, the simplified Reynolds equations may be valid [3] [4]. On the other hand, if the Reynolds number is low, and the ratio of amplitude to gap width is small, a perturbation from the Couette flow case is successful [5] [6]. If the Reynolds number is zero and the protuberances are periodic vertical fins, an eigenfunction expansion and matching method can be used [7]. No literature—theoretical, numerical, or experimental—exists for finite protuberances at finite Reynolds numbers. The aim of the present paper is to study the flow between the relative motion of a smooth surface over a rough surface with saw-tooth grooves. The size of each protuberance is of the same order as the mean gap width between the surfaces. This situation occurs when the moving surfaces are close together. The nonlinear Navier-Stokes equations will be used and due to the complicated boundary condition, all previous methods fail.

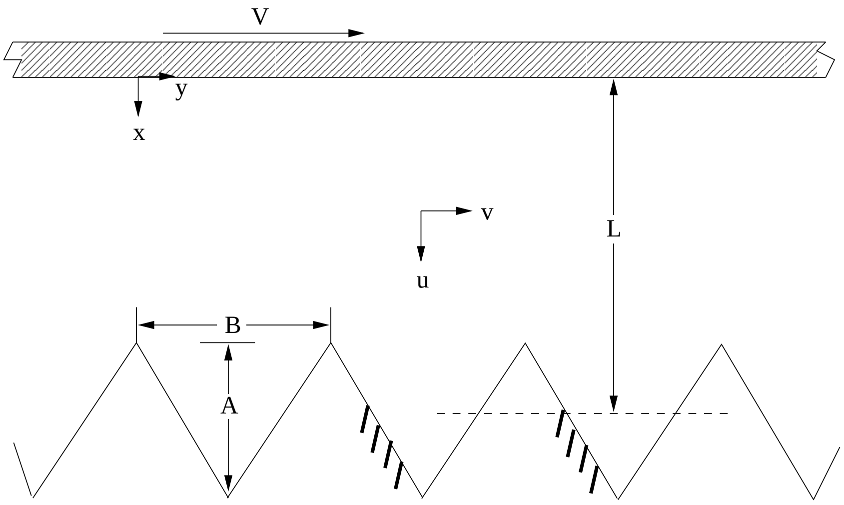

Fig. 1. The geometry.

2. FORMULATION

Fig. 1 shows the cross section. A top smooth flat surface is moving in its own plane with velocity V. The bottom rough surface has saw-tooth corrugations with period B and height A. The mean gap width between the surfaces is L and this channel is filled with an incompressible fluid of kinematic viscosity ν. The sawtooth and the triangular grooves are assumed to be equilateral triangles in the present paper, although our method can be adapted to scalene triangular shapes.

We normalize all lengths by L and all velocities by V. Then the height of the triangles is $a \equiv A/L$ and the period becomes $b = 2a/\sqrt{3}$. Let (u, v) be the velocity components in the (x, y) directions shown in Fig 1. The 2D incompressible Navier-Stokes equations are

$$uu_x + vu_y = -p_x + R(u_{xx} + u_{yy}), \tag{1}$$

$$uv_x + vv_y = -p_y + R(v_{xx} + v_{yy}), \tag{2}$$

$$u_x + v_y = 0, \tag{3}$$

where R is the Reynolds number VL/ν, and p is the normalized pressure. Define a stream function ψ such that $(u, v) = (\psi_y, -\psi_x)$. Then the Navier-Stokes equations can be written in the form

$$\zeta_{xx} + \zeta_{yy} - R\psi_y\zeta_x + R\psi_x\zeta_y = 0, \tag{4}$$

where $\zeta(x, y)$ is the vorticity

$$\zeta = \psi_{xx} + \psi_{yy}. \tag{5}$$

The advantage of this formulation is that the order of the PDEs is two, which allows us to use existing elliptic PDE solving software. In contrast, the stream function only formulation of the problem is a fourth order PDE. However, we have to provide additional boundary conditions in order to determine the vorticity.

3. BOUNDARY CONDITIONS

The downside of using the stream-vorticity formulation of the problem is that we need two boundary conditions on each boundary. Moreover, this forces us to solve a coupled system, which includes both unknown functions, because we do not have explicit boundary conditions for vorticity. That is, we impose on each surface one Dirichlet and one Neumann boundary condition on the stream function.

On the bottom (rough) surface, the boundary conditions are obtained from the physical "no slip" constraint ($u = v = 0$):

$$\begin{aligned} \psi(x, y) &= 0, \\ \frac{\partial \psi}{\partial n}(x, y) &= 0, \end{aligned} \tag{6}$$

where n denotes the direction normal to the surface.

On the top surface, the Neumann boundary condition is easy to impose, and is obtained from the condition that the lateral velocity is one ($v = 1$):

$$\frac{\partial \psi}{\partial x}(x, y) = -1. \tag{7}$$

However, the Dirichlet boundary condition on the top surface is peculiar: we know that the stream function is constant along this surface, but we do not know the value of the constant. Denoting by ψ_0 the constant (but unknown) value of ψ on the top surface, our Dirichlet-type boundary condition is

$$\psi(x, y) = \psi_0. \tag{8}$$

The value of ψ_0 is determined by the zero-pressure-gradient condition. That is, we require that the pressure be periodic and thus the same at $y = 0$ and $y = b$. The pressure periodicity is expressed by the integral equation:

$$\int_0^b \frac{\partial p}{\partial y}(0, y)\, dy = 0.$$

Since from Equation (2)

$$\frac{\partial p}{\partial y}(0, y) = -R[\psi_{xxx}(0, y) + \psi_{yyx}(0, y)],$$

we get

$$\int_0^b [\psi_{xxx}(0, y) + \psi_{yyx}(0, y)]\, dy = \int_0^b \zeta_x(0, y)\, dy = 0. \tag{9}$$

The boundary conditions for the channel are obtained by assuming periodicity, i.e.,

$$\psi(x, 0) = \psi(x, b), \qquad \zeta(x, 0) = \zeta(x, b), \tag{10}$$

$$\frac{\partial \psi}{\partial y}(x, 0) = \frac{\partial \psi}{\partial y}(x, b), \qquad \frac{\partial \zeta}{\partial y}(x, 0) = \frac{\partial \zeta}{\partial y}(x, b), \tag{11}$$

for $0 \leq x \leq 1 - a/2$.

Altogether, Equations (6–11) represent the set of boundary conditions.

4. NUMERICAL SOLUTION

Our numerical solution strategy is characterized by the following:

1. We solve one linear system of coupled unknowns, ψ and ζ, for the reasons discussed in Section 2.
2. We perform linearization before discretization. That is, we linearize Equation (4) as follows:

$$\zeta_{xx} + \zeta_{yy} - R\psi_y^{i-1}\zeta_x + R\psi_x^{i-1}\zeta_y + R\zeta_y^{i-1}\psi_x - R\zeta_x^{i-1}\psi_y = R(\psi_x^{i-1}\zeta_y^{i-1} - \zeta_x^{i-1}\psi_y^{i-1}), \quad (12)$$

   where the superscript $i-1$ refers to the known solution from the previous step. So, we solve the linear PDE consisting of Equations (5) and (12), together with boundary conditions (6–11).
3. We discretize using collocation, approximating the unknown functions with piecewise bicubic polynomial basis functions, also known as Hermite bicubics. This choice of discretization method is attractive because of its high accuracy—$O(h^4)$ discretization error on smooth problems—compared with standard finite difference or finite element approaches.

Discretization and iteration. Our code is based on the ELLPACK [9] package for solving elliptic PDEs. ELLPACK is a complete system, including support for problem definition, discretization, and linear system solution. Our code extends ELLPACK's *general domain collocation* discretization module [10] in several ways. Specifically, the major extensions are:

1. Solve a system of two coupled PDEs, rather than one PDE.
2. Support periodic boundary conditions for nonrectangular domains. Our modification is specific to the present problem, supporting only the periodic boundary conditions (10–11) across the channel. This is actually achieved by identifying the bicubic basis functions centered at $(x, 0)$ with those centered at (x, b). Because the Hermite bicubics are only C^1, higher order derivatives of the collocation approximation are not necessarily periodic.
3. Support the integral boundary condition (9) along with the special Dirichlet boundary condition (8) along the top surface.

The first and second extensions involved major re-coding of the discretization module. The last change involves including the value of ψ_0 as an extra unknown in the Dirichlet-like boundary equations on the top surface and expressing the pressure gradient equation in terms of ψ and ζ. The integral (9) is computed using Simpson's rule. We remark that using Hermite bicubic basis functions implies that no truncation error is caused by Simpson's rule.

Our modified discretization code is called from a main program that contains two iterations: an outer iteration on R and an inner Newton iteration on the linearized problem. The stopping criterion for the Newton iteration requires that the infinity norm of the difference between two consecutive iterates, ψ^i and ψ^{i-1}, be less than $\epsilon = 10^{-7}$. Each Newton iteration uses as initial guess the solution computed in the previous outer iteration.

Grid design. We have employed a quasi-uniform mesh with local mesh refinement around the tips of the sawtooth surface. Denote the uniform grid spacing along, and perpendicular to, the top surface by H_y and H_x, respectively. Let $w = 1 - a/2$ be the width of the channel between the top surface and the tips of the bottom sawtooth surface. The grid is obtained in terms of a resolution parameter, m, and a refinement parameter, k, as follows:

1. Place $2m + 1$ vertical grid lines, with spacing $H_y = b/2m$.
2. Place $m+1$ horizontal grid lines, with spacing $H_x = a/m$, ranging from $x_1 = w$ to $x_2 = w + a$.
3. Place $m' = \max\{\lceil w/H_x \rceil, 2\}$ horizontal grid lines, with spacing $H'_x = w/m'$, in the interval $x_0 = 0$ to $x_1 = w$.

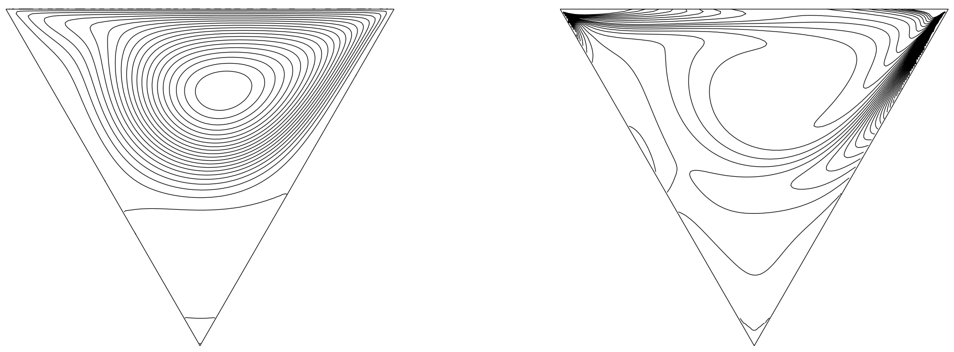

(a) (b)

Fig. 2. The case when the two surfaces touch ($a = 2$), $R = 200$.
(a) Streamlines, (b) constant vorticity lines.

4. Locally refine the grid by adding k horizontal grid lines: one additional grid line subdividing the interval $(x_1 - H_x', x_1)$, and $k-1$ lines equally spaced in the interval $(x_1, x_1 + H_x)$.

The refinement parameter $k = 3$ is used for all the numerical results reported in subsequent sections. Different values of the grid parameter m are used for different values of sawtooth height a: we use $m = 30$ for $a = 2$, $m = 25$ for $a = 1.8$, and $m = 20$ for $a = 1.2$ and 0.8. With these choices, the Newton iteration converges in at most 4 iterations for $R \leq 1000$. It is noted that these values of the grid parameters result in a discrete problem of approximately 10,000 equations and unknowns. The linear systems of equations are solved with band Gaussian elimination.

Convergence study. We ensure the accuracy of the inner iteration through the upper bound ϵ on the infinity norm of the difference between consecutive Newton iterations. The overall accuracy in solving the PDE is estimated using a grid convergence approach.

The idea is to compare the numerical solutions on increasingly finer grids, which provide increasingly accurate numerical solutions. This allows one to estimate the accuracy in a coarse grid solution in terms of the change in the numerical solution when moving from the coarse grid to the fine grid. Formally, let ψ be the true stream function and let ψ_c and ψ_f be the numerical solution on a coarse and fine grid respectively. All these functions are evaluated on a reference grid. If $\|\psi_f - \psi\| < \|\psi_f - \psi_c\|$, where $\|\cdot\|$ denotes the infinity norm, we get:

$$\|\psi_c - \psi\| \leq \|\psi_c - \psi_f\| + \|\psi_f - \psi\| < 2\|\psi_c - \psi_f\|.$$

Thus $2\,\|\psi_c - \psi_f\|$ is an upper bound on $\delta = \|\psi_c - \psi\|$. Applying this method for $a = 1.2$, where the coarse grid has $m = 20$, which gives a 31×45 mesh, and the fine grid has $m = 25$, which gives a 38×55 mesh, the upper bounds on $\delta/\|\psi_c\|$, for $R = 0$, 500, and 1000, are $0.017, 0.025$, and 0.029, respectively.

5. STREAMLINES AND VORTICITY

When a=2, or when the top moving flat surface just touchs the tips of the bottom sawtooth surface, the problem becomes the flow in a triangular cavity with one side moving. Our current numerical code generates results identical to those of [8]. Typical streamlines for $R = 200$ are shown in Fig. 2a, where we note at least three recirculating cells. The center of the dominant cell is skewed towards the direction of the moving side. Fig. 2b shows the corresponding vorticity. The

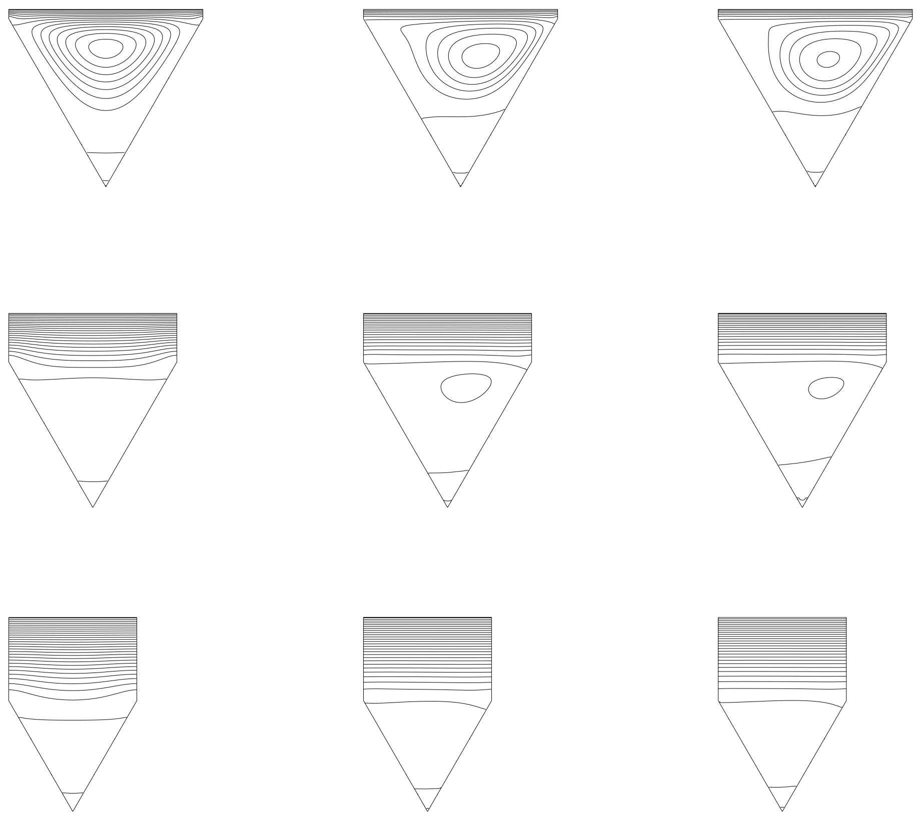

$(w = 0.1)$

$(w = 0.4)$

$(w = 0.6)$

Fig. 3. Streamline patterns. First column $R = 0$, second column $R = 500$, third column $R = 1000$. First row $a = 1.8$, second row $a = 1.2$, third row $a = 0.8$.

highest vorticity is produced at the corners of velocity discontinuity, then transported downstream. Of course, the zero-gap width case gives infinite drag on the moving top surface and we shall no longer be concerned with the cavity problem except for the comparison with [8].

Fig. 3 shows the streamlines for various different sawtooth heights, a, and different Reynolds numbers, R. We see that at $R = 0$, the streamlines are symmetric fore and aft, and when R is increased, the recirculating flow becomes weaker and skewed. The effect of a smaller height a (or larger distance between the surfaces) is to strengthen the almost parallel Couette-like through flow and weaken the recirculating flow. The dividing line between the through flow and the dominant recirculation is also depressed downward into the trough. Notice the dip of the dividing line at the windward side of the sawtooth. Fig. 4 shows the corresponding vorticity lines. We see the vorticity is the strongest at the exposed tips of the sawtooth. It is also transported along the streamlines. At a high Reynolds number and a small gap width, a constant vorticity core is developed, similar to the cavity problem (Fig. 2b). However for a smaller a (or larger gap width), there is no such constant vorticity core, perhaps due to the fact that the local Reynolds number is not sufficiently large.

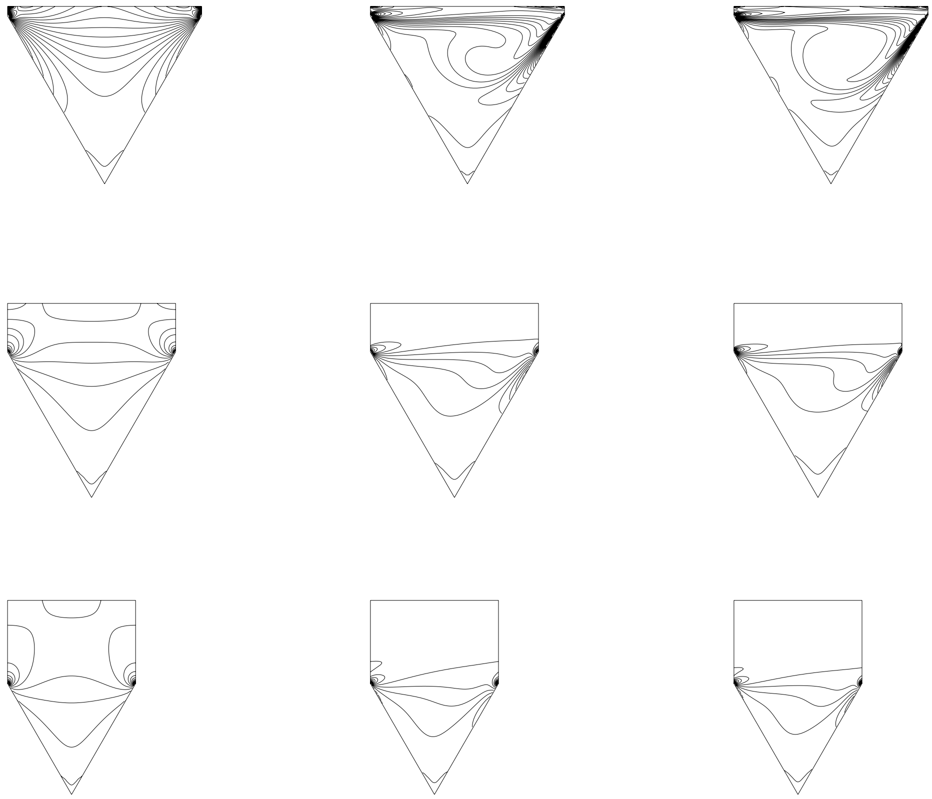

Fig. 4. Constant vorticity lines. Same legend as Fig. 3.

6. DRAG

The drag per area on the top surface is proportional to the mean shear stress. Let D denote the drag per area normalized by uV/L. Then

$$D = \frac{-1}{b}\int_0^b \left.\frac{\partial v}{\partial x}\right|_{x=0} dy = \frac{1}{b}\int_0^b \left.\frac{\partial^2 \psi}{\partial x^2}\right|_{x=0} dy = \frac{1}{b}\int_0^b \zeta|_{x=0}\, dy. \tag{13}$$

For a smooth bottom surface, Couette flow prevails and $D = 1$. For a sawtooth bottom surface, the result from Equation (13) is depicted in Fig. 5 for various Reynolds numbers and sawtooth height a. We observe the following:

1. Drag increases dramatically with sawtooth height a, being 1 at $a = 0$ and approaching infinity as $a \to 2$.
2. Drag increases with Reynolds number; the increase is larger for larger amplitude of the bottom corrugations.

CONCLUSIONS

The determination of the effect of surface corrugations (roughness) on hydrodynamic lubrication is indeed important but difficult. In many situations the amplitude of the corrugations is of the same order as the period and the gap width, causing the simplified lubrication theory or perturbation theory to be inapplicable. This problem is now numerically solved for arbitrary amplitudes using the full Navier-Stokes equations. The method of collocation—based on Hermite bicubic basis

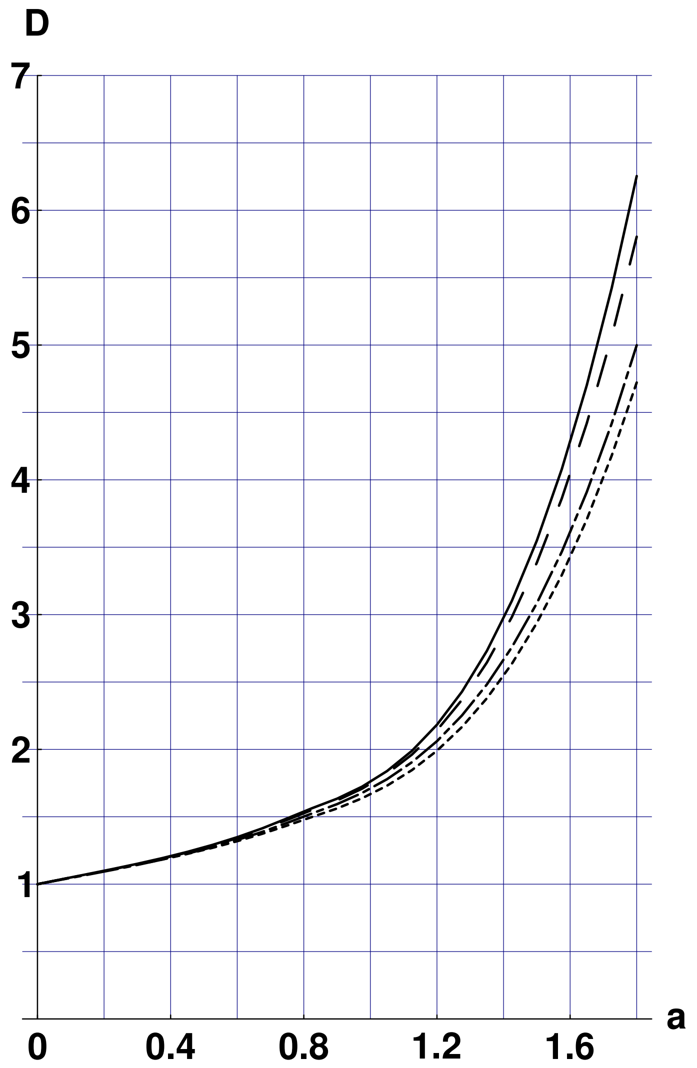

Fig. 5. The normalized drag versus depth of sawtooth a for Reynolds numbers $R = 1000$ (solid), $R = 500$ (dashed), $R = 100$ (dash-dot), and $R = 0$ (dotted).

functions, a locally refined mesh, and carefully chosen collocation points—is sufficiently flexible to handle the complicated boundary conditions and irregular geometry required to numerically solve this problem.

Finite corrugations may increase the drag several fold over the traditional Couette value. Even though the mean gap width and thus the total fluid volume is the same, streamline studies show that corrugations decrease the effective gap width, thus causing higher resistance. Fig. 5 should be very useful in the design of lubrication components.

REFERENCES

1. J. A. Schey, *Tribology in Metalworking—Friction, Lubrication, and Wear*, American Society for Metals, Metals Park, Ohio (1983).
2. A. E. Bergles, Some perspectives on enhanced heat transfer—second generation heat transfer technology, *J. Heat Trans.*, **110**, 1082 (1988).
3. H. Schlichting, *Boundary Layer Theory*, 7th Ed., McGraw-Hill, New York (1979).
4. H.G. Elrod, Thin-film lubrication theory for Newtonian fluids with surfaces possessing striated roughness or grooving, *J. Lub. Tech.*, **95**, 484 (1973).

5. C.Y. Wang, Drag due to a striated boundary in slow Couette flow, *Phys. Fluids*, **21**, 697 (1978).
6. P. Disimile and C.Y. Wang, The forces due to the relative motion of two corrugated plates, *Phys. Fluids*, **26**, 611 (1983).
7. C.Y. Wang, The Stokes drag due to the sliding of a smooth plate over a finned plate, *Phys. Fluids*, **6**, 2248 (1994).
8. C.J. Ribbens, L.T. Watson, and C.Y. Wang, Steady viscous flow in a triangular cavity, *J. Comp. Phys.*, **112**, 173 (1994).
9. J.R. Rice and R.F. Boisvert, *Solving Elliptic Problems Using ELLPACK*, Springer-Verlag, New York (1985).
10. E.N. Houstis, W.F. Mitchell, and J.R. Rice, Collocation software for second-order elliptic partial differential equations, *ACM Trans. Math. Softw.*, **11**, 379 (1985).